Biosensors and Bioelectronics 122 (2018) 37–42

Contents lists available at ScienceDirect

Biosensors and Bioelectronics

journal homepage: www.elsevier.com/locate/bios

A photoelectrochemical sensor for highly sensitive detection of amyloid beta based on sensitization of Mn:CdSe to Bi_2WO_6/CdS

Rui Xu[a], Dong Wei[a], Bin Du[a], Wei Cao[a], Dawei Fan[a], Yong Zhang[a,*], Qin wei[a], Huangxian Ju[a,b]

[a] Key Laboratory of Interfacial Reaction & Sensing Analysis in Universities of Shandong, School of Chemistry and Chemical Engineering, University of Jinan, Jinan 250022, PR China

[b] State Key Laboratory of Analytical Chemistry for Life Science, Department of Chemistry, Nanjing University, Nanjing 210023, PR China

ARTICLE INFO

Keywords:
Photoelectrochemical sensor
Competitive-type
Bi_2WO_6
Mn:CdSe
Amyloid beta

ABSTRACT

A high sensitivity photoelectrochemical (PEC) immunosensor for amyloid beta (Aβ) detection, which has great neurotoxic effect on the progression of Alzheimer's disease (AD), was presented based on the sensitization of Mn^{2+} doped CdSe (Mn:CdSe) to Bi_2WO_6/CdS electrode. Bi_2WO_6 was synthesized successfully with a unique flower-like amorphous structure, providing a merit to load functional CdS for obtaining an expected PEC response. Mn:CdSe was used to label Aβ for acquiring Mn:CdSe-Aβ bioconjugate and enhancing the detection sensitivity via the competitive immunoreaction of Mn:CdSe-Aβ and Aβ with antibody immobilized on Bi_2WO_6/CdS electrode. The doped of Mn^{2+} in CdSe nanoparticles could induce energy defect that impeded the recombination of photo-generated charges, and greatly enhanced PEC response for ultrasensitive detection of Aβ. The proposed immunosensor for Aβ showed a linear range of 0.2 pg mL^{-1}–50 ng mL^{-1} with a detection limit of 0.068 pg mL^{-1}, also with good stability, high selectivity, and acceptable reproducibility. The sensitization of Mn:CdSe provided a new way for preparation of highly sensitive protein biosensors.

1. Introduction

Alzheimer disease (AD), a chronic degenerative disease of the central nervous system, is the most common type of dementia in the elderly (Meda et al., 1995; Mustafa et al., 2010; Rushworth et al., 2014). The manifestations of AD were mainly manifested in cognitive dysfunction, progressive memory disorders, personality changes, language disorders, and other neuropsychiatric symptoms (Kaushik et al., 2016; Qin et al., 2018). It has become one of the most fatal factors threatening the human life and health, and its incidence rate has been increasing year by year. The abnormal aggregates of beta amyloid (Aβ (1 − 42)) peptides in brain was considered to be a momentous role in the etiology of AD (Andreasen et al., 1999). Hence, there was a continuing demand for fast and simple analysis the determination of Aβ. Various techniques and attempts have been made in the past to developed new methods for Aβ (1 − 42) detection, including electrochemical methods (Carneiro et al., 2017), enzyme-linked immunosorbent assay (Barghorn et al., 2005), electrochemical luminescence (Ke et al., 2017), atomic force microscopy (Caballero et al., 2015), and fluorescence spectroscopy (Liu et al., 2017) et al. These methods have achieved relatively satisfactory results.

As a new fashioned analytical method for biomolecules detection, photoelectrochemical (PEC) immunosensing own the merits of high selectivity on account of the unique form of signal change. In addition, it's simple, have low-cost, and fast analyzing speed (Zang et al., 2017; Zhang et al., 2013; Zhao et al., 2017). Moreover, many photosensitive materials bas been applied into the construction of PEC immunosensors , such as bismuth-based oxides including BiOBr (Fan et al., 2017), BiOI (Sun et al., 2015), Bi_2O_3(Jiang et al., 2013), $BiVO_4$(Su et al., 2011; Wetchakun et al., 2012) and $BiYWO_6$(Han et al., 2018) et al., have aroused great interest in both photochemistry and photobiology. As a significant semiconductor material with superb properties, bismuth tungstate (Bi_2WO_6) has appealed great attention in many research fields, thanks to its high stability, non-toxicity, suitable band gaps, and good photocatalytic activity (Amano et al., 2011; Chen et al., 2017). However, it was rarely applied to PEC field owing to the truth that the rapid recombination of photo-generated electron–hole (e^-/h^+) pairs, which significantly restrict the energy-conversion efficiency. This limitation can be settled by the sensitization of other photosensitive materials such as CdS, a popular sensitizer (Wen and Ju, 2016) with excellent visible-light absorption ability (Wei et al., 2017; Zang et al., 2016), and easy availability (Xu et al., 2016; Zhao et al., 2012). As one type of semiconductor nanocrystals, CdSe with broad excitation spectrum, good photo stability and favorable PEC properties

* Corresponding author:
E-mail address: yongzhang7805@126.com (Y. Zhang).

https://doi.org/10.1016/j.bios.2018.09.030
Received 18 July 2018; Received in revised form 7 September 2018; Accepted 8 September 2018
Available online 10 September 2018
0956-5663/ © 2018 Elsevier B.V. All rights reserved.

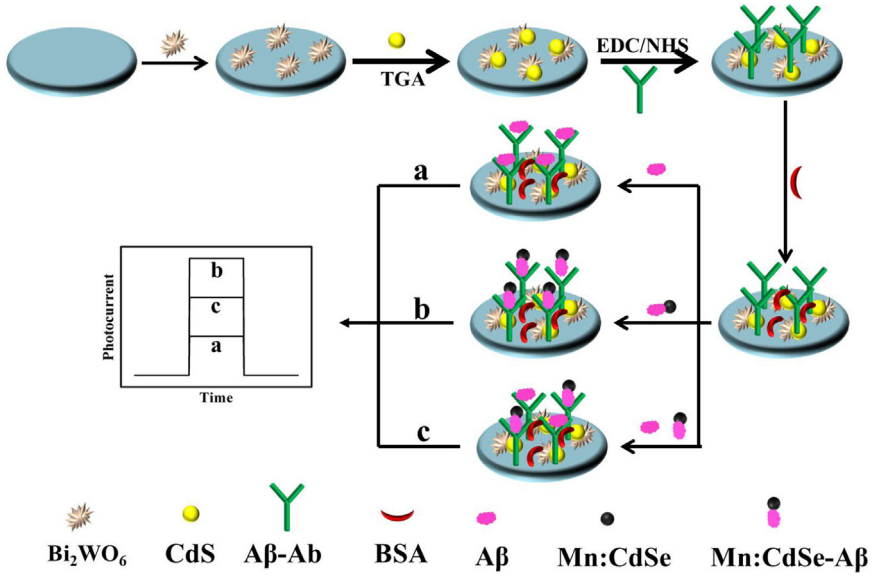

Scheme 1. Fabrication process of photoelectrochemical immunosensor.

(Li et al., 2016; Liu et al., 2009; Wang et al., 2014) has attracted wide attention in PEC as well as biomedical field. The recombination of photo-generated e^-/h^+ pairs can be effectively suppression by hybridizing materials with metallic ions (Zhao et al., 2016), which also control the crystalline phase and size of the resulting materials (Tian et al., 2012).

To develop sensitive PEC biosensor for Aβ detection, herein, Mn doped CdSe composites (Mn:CdSe) with stable and strong PEC signals were synthesized as an sensitizing material to label Aβ. The doped Mn^{2+} could produce an electronic state in the mid-gap region of CdSe crystal which led to separation of the photogenerated e^-/h^+ pairs (Gu et al., 2017; Zhang et al., 2017), thereby increasing the PEC response. After the Aβ antibody was immobilized on Bi_2WO_6/CdS modified ITO electrode (Scheme 1) to obtain the PEC immunosensor for Aβ (1 − 42), different concentrations of target Aβ and Mn:CdSe-Aβ mixture were incubated to perform a competitive immunoreaction. The proposed PEC immunosensor exhibited ultrahigh sensitivity, satisfactory reproducibility, and acceptable specificity.

2. Experimental section

2.1. Reagents and apparatuses

The ITO conductive glass was acquired from Zhuhai Kaivo Electronic Components Co. Ltd., China. Aβ antigen (Ag) and Aβ antibody (Ab) were gained from Biocell Science Co. Ltd., (Shanghai, China). Other details were displayed in Supplementary materials.

2.2. Preparation of Bi_2WO_6

Bi_2WO_6 was prepared with an ordinary hydrothermal method similar to the previous reference with slight modification (Amano, 2008). First, 2.75 mmol of sodium tungstate dihydrate ($Na_2WO_4{\cdot}2H_2O$) was dissolved into 30 mL of ultrapure water, as solution A. Then, 5.0 mmol of bismuth nitrate pentahydrate ($Bi(NO_3)_3{\cdot}5H_2O$) was dispersed in 20 mL of ultrapure water, as solution B. After mixed solution A and solution B along with violent magnetic stirring, the mixture was stirred for another 10 min and then sonicated for 20 min at room temperature, followed by pouring into a dry Teflon-lined autoclave, and reacted at 160 °C for 20 h. Afterward, the autoclave was allowed to cool naturally, the product was washed with anhydrous ethanol and ultrapure water for several times, respectively, and then the precipitate was dried at 60 °C.

2.3. Preparation of Mn:CdSe nanoparticles

Mn:CdSe nanoparticles were synthesized according to our previous report with same modification (Wang et al., 2017). Firstly, the processes of NaHSe precursor prepared were as follows: 0.7497 mmol Se power was added into 5 mL ultrapure water with vigorous stirring under argon atmosphere, then 10.56 mmol sodium borohydride ($NaBH_4$) was added into the solution continue with stirring. Coinstantaneous, 0.3997 mmol cadmium chloride hydrate ($CdCl_2{\cdot}2.5H_2O$) and 0.0113 mmol manganese(II) chloride ($MnCl_2$) were dispersed into 20 mL ultrapure water, then 0.056 mL MPA (3-mercaptopropionic acid) was added with violent stirring for 10 min. Later, using 0.5 mol L^{-1} NaOH solution adjusted the pH value to 9. Afterwards the NaHSe precursor was quickly poured into the above solution with continuous stirring for another 30 min, and then transferred to a Teflon-lined autoclave, reacting at 160 °C for 40 min. Finally the product was washed with ultrapure water and ethanol for several times and dried in vacuum.

2.4. Preparation of Mn:CdSe-Aβ bioconjugates

5 mg of as-prepared Mn:CdSe nanoparticle was dispersed in PBS (pH 7.4), then 10 μL of 5 mg mL^{-1} EDC and 10 μL of 1 mg mL^{-1} NHS were added into the solution, the mixture was activated for 15 min at room temperature. Subsequently, 600 μL of Aβ (1 ∼ 42) solution (10 μg mL^{-1}) was added up to the solution and incubated gently at 35 °C for 3 h, then placed overnight under 4 °C. After that, washing the mixture with PBS (pH = 7.4). Finally, the product was dissolved into 2 mL PBS (pH = 7.4), and stored at 4 °C for later use.

2.5. Fabrication of PEC sensor

The PEC immunosensor was fabricated on diced ITO pieces (0.9 cm × 2.0 cm). Prior to the modification, the ITO electrode was ultrasonic cleaning with acetone, ethanol and thrice-ultrapure water for about 30 min, successively, followed by drying with nitrogen. First, the bare ITO was modified with 6 μL Bi_2WO_6 solution (5 mg mL^{-1}), and dried unaffectedly on environment atmosphere, followed by calcination at 400 °C for 1 h in air steam. Then 6 μL of CdS solution (5 mg mL^{-1}) was dropped on the electrode and dried at room temperature to form a Bi_2WO_6/CdS modified electrode (Scheme 1). After the got-up electrode

was immersed in 3 mmol L^{-1} TGA (thioglycollic acid) solution for assembly of TGA, and rinsing with ultrapure water, then 6 μL of mixed solution (containing 20 mg mL^{-1} EDC and 10 mg mL^{-1} NHS) was embellished on the ITO/Bi_2WO_6/CdS electrode for 40 min at room temperature. Once the electrode dried, 6 μL of Ab was assembled onto the surface of electrode and incubated at 4 °C for 40 min. After being washed, 3 μL of BSA (1 w %) was dropped on the electrode to erase nonspecific binding and block the possible excess active sites. After rinsed, the electrode was incubated with 6 μL of mixture (3 μL of Mn:CdSe-Aβ and 3 μL of different concentrations of Aβ (1 − 42)) for 40 min. Finally the electrode was rinsed with ultrapure water and ready to be used for PEC measurements.

2.6. Detection of real samples

Real sample analysis is vital in immunosensor for target detection (Ren et al., 2017a, 2017b; Xing et al., 2018; Yang et al., 2017). Human serum samples were obtained from the hospital of University of Jinan (Jinan, China). Before the analysis, the simples were attenuated with PBS (pH = 7.4) until a level within the calibration range. After determined the obtained samples, the PEC signals of serum samples spiked with 0.05, 0.50 and 5.00 ng mL^{-1} were also obtained. The PEC signal was measured at room temperature in 10 mL of PBS (pH 7.4) containing 0.1 mol L^{-1} AA in a conventional electrochemical cell with saturated calomel electrode (SCE) as a reference electrode and platinum electrode as the counter electrode. A LED lamp (450 nm) was utilized as excitation light and switched on and off every 20 s under 0 V potential (vs. SCE).

3. Results and discussion

3.1. Characterization of synthesized materials

The characters of crystalline structure of Bi_2WO_6 were performed by X-ray diffraction (XRD) patterns. Several sharp peaks were found at 2θ = 28.3°, 32.9°, 47.1°, 56.0° and 58.5° (Fig. 1A), which corresponded to the (131), (002), (202), (133), and (262) planes. The morphology of Bi_2WO_6 was a three-dimensional flower-like structure assembled from nanosheet (Fig. 1B), which possessed large specific surface area for loading more CdS nanoparticles to produce a good photocurrent signal (Wang et al., 2018). The scanning electron microscopy (SEM) pattern in Fig. 1C depicted that CdS was successfully modified on Bi_2WO_6. Fig. S1 showed the pattern of CdS, it was a quasi-spherical nanoparticle with size around 20 nm, which was suitable for combining with the large-size Bi_2WO_6. The transmission electron micrographs (TEM) image of Mn:CdSe (Fig. 1D) showed a uniform nanospheres, and it contained the elements of only Mn, Se and Cd (Fig. 1E), confirming the successful formation of Mn:CdSe composite. The UV–vis reflectance spectra of Bi_2WO_6/CdS/Mn:CdSe showed a wide and superb absorption to visible light (Fig. 1F), illustrating that the sensitization of Mn:CdSe improved the absorption of composite to visible light.

3.2. Possible PEC mechanism of immunosensassay

The possible light-induced electrons transfer process of the immunosensor was put forward in the environment of PBS electrolyte containing AA. As displayed in Scheme 2, under visible light illumination, the low photocurrent produced by Bi_2WO_6 due to the narrow band gap, which led to rapid recombination of photo e^-/h^+. Fortunately, CdS as an excellently semiconductor has the matched band energy level with Bi_2WO_6, herein, the Bi_2WO_6 was modified with CdS to acquire Bi_2WO_6/CdS composites, which could produce superb efficiency of the visible light. Meanwhile, for the sake of improving the sensitivity of immunosensor, Mn:CdSe was used as a probe labeled on Aβ (1 − 42) antigen. There are effective energy level matching between CdS and CdSe, which facilitated charge separation owing to the quick electron transfer, thus amplified the PEC response. The doping of Mn^{2+} could induce energy defect, which could suppress the recombination of photo-generate charges (Fig. S2 showed the PEC response of different electrodes). Owing to the matching band energy level between Mn:CdSe and CdS, the photo-generated electrons could transfer to the conduction band (CB) of CdS, then they could transfer to the CB of Bi_2WO_6. At the meantime, AA as a superior electron donor (Kang et al., 2010b), it could combined with photo-generated holes that hinder the recombination of photo-generated electrons and holes, resulting the increased of photocurrent signals. It was notable that the CB and valence band (VB) edges of Bi_2WO_6, CdS and Mn:CdSe were gradually increased beneficial to transfer of photo-generated carriers. Therefore, a PEC sensor was successfully constructed with superb visible light performance.

3.3. Analytical performance of the PEC immunosensor

By detecting PEC signals of electrodes modified with different materials, the photocurrent curves were obtained for the characterization of PEC behavior. Obviously, the bare ITO electrode showed negligible PEC signal (Fig. 2A, curve a), and Bi_2WO_6 modified ITO showed increasing photocurrent (Fig. 2A, curve b) and calcination could improve the response because Bi_2WO_6 would be more tightly adhesion onto the ITO electrode (Liang et al., 2015; Ong et al., 2013)(Fig. S3). After loading CdS on Bi_2WO_6 modified ITO, the strongest PEC signal was obtained due to the matched energy band level (Fig. 2A, curve c). With the layer by layer modification of Ab (curve d), BSA (curve e), the photocurrent showed a down trend because of the bioactive substances was non-conducting that would hinder the electrons transfer. However after the mixture of Aβ and Mn:CdSe-Aβ bioconjugates was bound to the immobilized Ab, the electrode exhibited an distinct enhanced photocurrent response (curve f). The results indicated that the PEC immunosensor was successfully constructed.

To better understand the interfacial feature of the proposed PEC sensor, the electrochemical impedance spectroscopy (EIS) was applied to prove the construction process (Liu et al., 2015). As displayed in Fig. 2B, the bare ITO exhibited a small resistance (curve a), which indicated a low resistance value of the redox couple. When the ITO was immobilized with Bi_2WO_6 (curve b) and CdS (curve c), the electrons transfer resistance value was increased on account of the poor conductivity of the semiconductor. The layer by layer modification of Ab (curve d), BSA (curve e), Mn:CdSe-Aβ bioconjugate (curve f) also increased gradually the resistance, indicating that protein molecules obstructed the electrons transfer.

3.4. Optimal conditions for the fabrication of PEC immunosensor

In order to obtain an ideal performance of the PEC sensor, the concentration of AA, the pH value of electrolyte solution, the concentration of Mn:CdSe, and the incubation time of Mn:CdSe-Aβ and Aβ mixture were evaluated in Fig. S4. Ascorbic acid (AA) was widely used in PEC testing to increase the PEC response because it was a great electron donor (Cong et al., 2016; Wang et al., 2009) and can be oxidized by the holes generated by illuminated Bi_2WO_6, CdS and Mn: CdSe to obstruct the combination of photo-generated e^-/h^+. Fig. S4 shown the comparative PEC measurement was operated in electrolyte solutions with AA and without AA, it was obvious saw that the PEC response was almost dozens of times larger in AA electrolyte than AA-free electrolyte. With the increasing concentration of AA, the photocurrent response increased, and achieved the optimum value when the concentration of AA was 0.1 mol L^{-1} (Fig. S5A). As the concentration of AA further increased, the photocurrent showed a downward trend, which might account for the saturation of electron donor. At higher AA concentration the decreased of photocurrent could be explained with the declined absorbance of electrolyte solution, which thus decreased the light intensity and formation efficiency of excited electron-hole center (Kang et al., 2010a). Thus 0.1 mol L^{-1} was selected as optimum

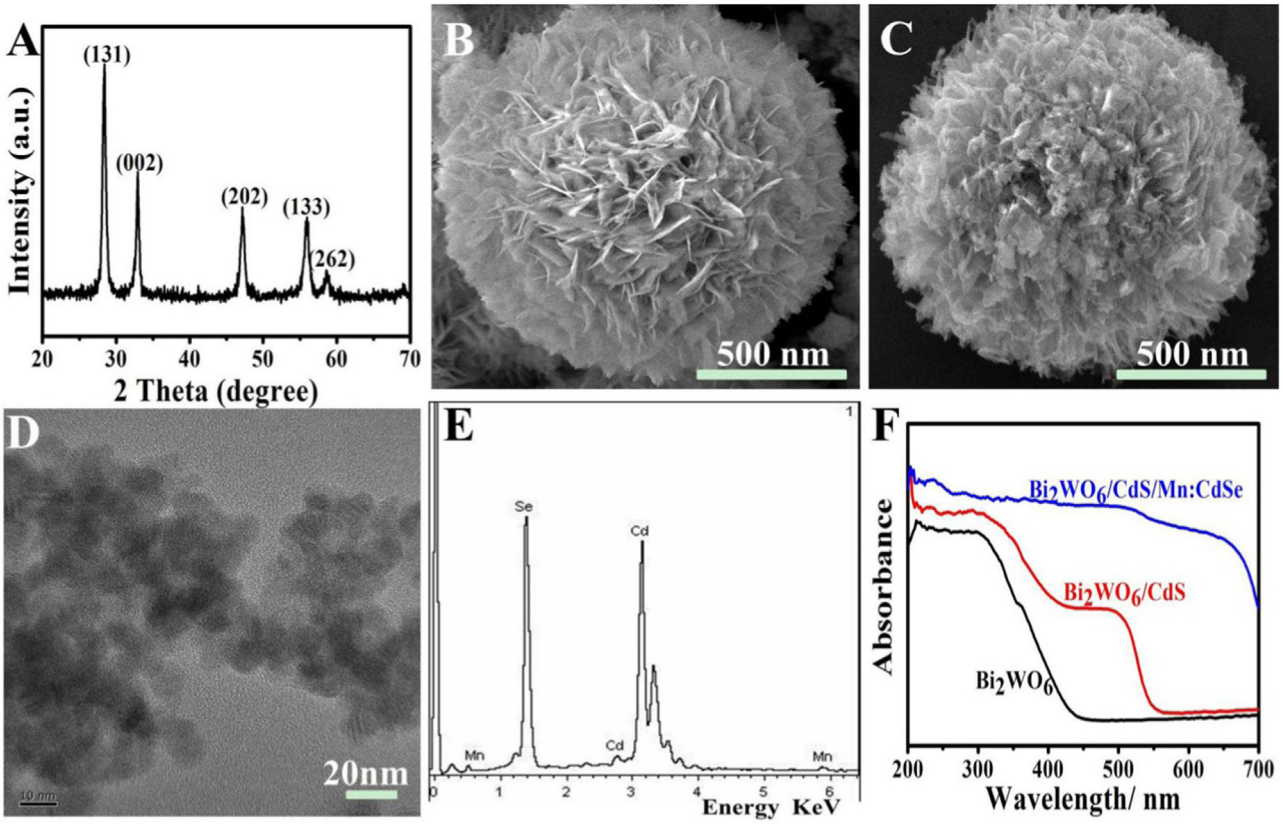

Fig. 1. (A) XRD image and (B) SEM image of Bi_2WO_6, (C) SEM image of Bi_2WO_6/CdS, (D) TEM image of Mn:CdSe, (E) EDS image of Mn:CdSe nanoparticles. (F) UV–vis diffuse reflectance spectra of Bi_2WO_6, Bi_2WO_6/CdS, Bi_2WO_6/CdS/Mn:CdSe.

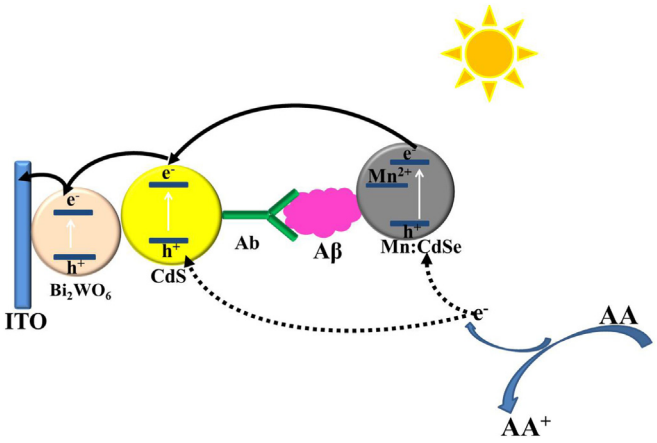

Scheme 2. Possible photogenerated electrons transfer mechanism of the immunosensor for target Aβ detection.

experimental condition. Fig S5B showed the effect of pH on the photocurrent intensity, as the pH increasing, the photocurrent gradually increased until the pH reached 7.4, which was similar with the physiological environment and fit for the activity of the immobilized protein. Hence the pH of 7.4 was the optimum value. Fig S5C demonstrated the effect of concentration of Mn:CdSe, the photocurrent gradually increased as the concentration of Mn:CdSe increased to 2.5 mg mL^{-1}, when the concentration of Mn:CdSe up to 3 mg mL^{-1}, the photocurrent had an decreased trend, demonstrating that too much Mn:CdSe was not stable for the detection. Therefore, 2.5 mg mL^{-1} was selected as the concentration of the marker. The photocurrent response gradually increased along with the incubation time of Mn:CdSe-Aβ and Aβ mixture up to 40 min and then tend to be stable at longer time (Fig. S5D), implying the immunoreaction was entirely finished on the electrode surface. Thus, 40 min was elected as the incubation time.

3.5. PEC determination of Aβ

Under the optimal experimental condition, the calibration curve of the proposed sensor was obtained, which was demonstrated in Fig. 3A. The linear correlation of photocurrent response with the logarithm of the Aβ concentration from 0.2 pg mL^{-1}–50 ng mL^{-1}, the regression equation was $I = 3.558–1.676 \log c_{A\beta}$ (ng mL^{-1}) and the correlation coefficient of 0.9967 (Fig. 3B). The detection limit (LOD, S/N = 3) was about to be 0.068 pg mL^{-1} calculated according to the literature (Yang et al., 2017), which is much lower than those of the similar detection. A comparison of the Aβ linear range and detection limit for the proposed PEC biosensor with the other similar configurations was shown in Table S1.

3.6. Reproducibility, stability and selectivity of the PEC immunosensor

Good reproducibility and stability was the general requirements for biosensors (Ren et al., 2018; Wu et al., 2018). In this work, for investigating the reproducibility of the sensor, several electrodes were embellished under the same conditions to test the photocurrent signal. As shown in Fig. 4A, the relative standard deviation (RSD) of the immunosensor was less than 4.61%, making that the fabricated PEC immunosensor had a great reproducibility clearly. To study the stability of the immunosensor, the time-dependent photocurrent switch of the electrode was supervised under reduplicative on/off visible light illumination. Fig. 4B indicates the photocurrent almost remain unchanged after 14 times on/off cycles. The result indicates that the designed immunosensor exhibited satisfied stability.

To further investigated the selectivity of the fabricated biosensor for

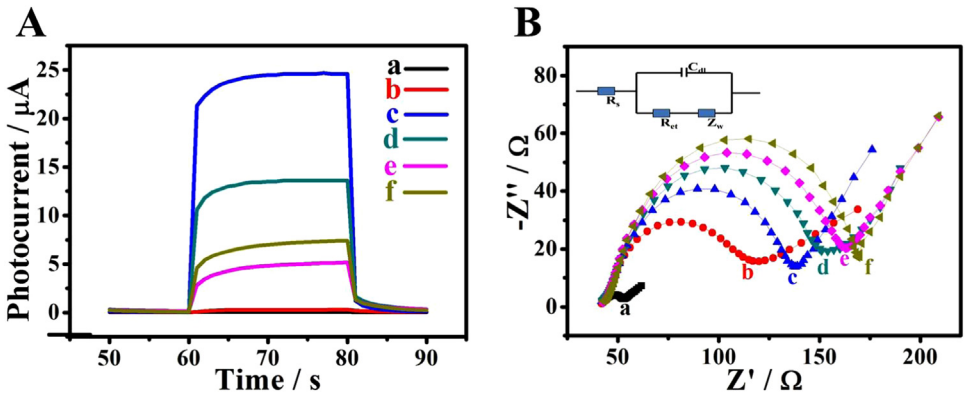

Fig. 2. (A) Photocurrent responses and (B) Nyquist diagrams of (a) the bare ITO electrode, (b) Bi_2WO_6/ITO, (c) CdS/Bi_2WO_6/ITO, (d) Ab/CdS/Bi_2WO_6/ITO, (e) BSA/Ab/CdS/Bi_2WO_6/ITO, (f) Aβ(5 pg mL^{-1}) + Mn: CdSe-Aβ/BSA/Ab/CdS/Bi_2WO_6/ITO. Inset of part B: the electrical equivalent circuit applied to fit the impedance spectra.

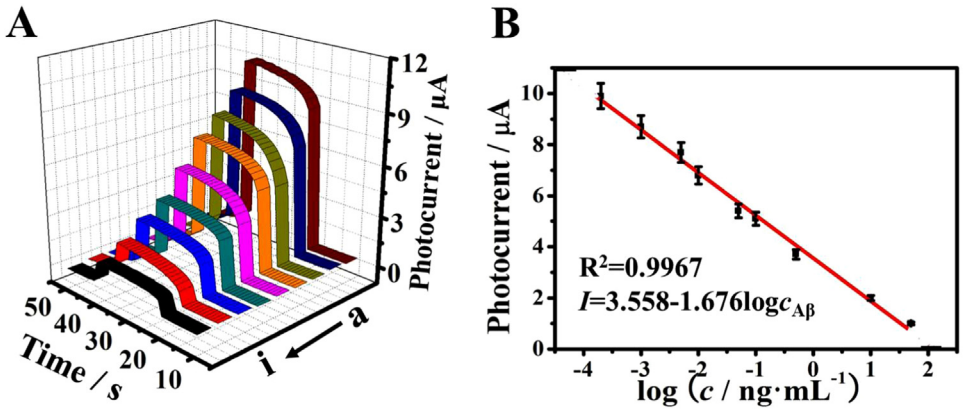

Fig. 3. (A) PEC response and (B) corresponding calibration curve of ITO/Bi_2WO_6/CdS/Ab/BSA electrode in the presence of mixture containing 3 μL of Mn: CdSe-Aβ bioconjugates and 3 μL of different concentrations of Aβ: (a-i) 0.0002, 0.001, 0.005, 0.01, 0.1, 0.5, 10 and 50 ng mL^{-1}, which were measured in phosphate buffer solution (pH 7.4) containing 0.1 M AA. Error bars = SD (n = 3).

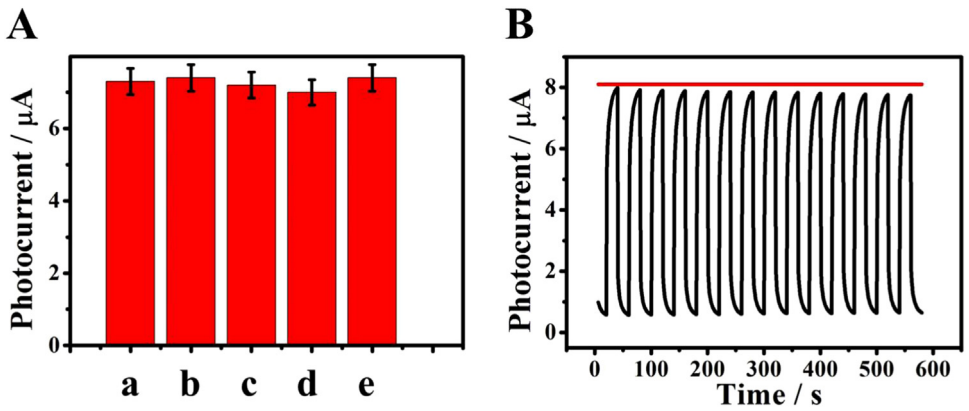

Fig. 4. (A) Stability test of the photoelectrochemical immunosensor, (B) Signal stability of photocurrent intensity for detection 5 pg mL^{-1} Aβ under for 14 cycles. Error bars = SD (n = 3).

Aβ detection, using some usual disturbed substance involving prostate specific antigen (PSA), insulin and CEA for interference experiments. As exhibited in Fig. S6, adding the amount of interfering substances was 100 times than Aβ, that the biosensor modified with or without 0.1 ng mL^{-1} Aβ, the PEC response exhibited a RSD of 1.78% and 4.34%, that proved the great specificity of the biosensor.

3.7. Real simple detection

For discussing the feasibility and accuracy of the proposed PEC immunosensor, different concentrations (0.05, 0.5 and 5 ng mL^{-1}) of the standard Aβ solution were added into serum samples, the experimental results were shown in Table S2. The average recovery rate of the immunosensor was in the range of 98.4–104.0%, and the RSD were 2.67–5.00%, illustrating the applicability of the proposed system for future clinical diagnosis development.

4. Conclusion

In short, a novel competitive type photoelectrochemical sensor was successfully fabricated for sensitivity detection of Aβ based on the sensitization of Mn:CdSe to Bi_2WO_6/CdS. Thanks to the three-dimensional flower structure of Bi_2WO_6, which provided a large specific surface to loaded functional CdS for obtaining the excellent photocurrent, creating an enabling environment for fabricating the sensor. By introducing Mn:CdSe-Aβ biocongujate in a competitive immunoreaction, a great sensitivity enhancement strategy was achieved rely on Mn:CdSe-Aβ, it would compete with Aβ to Aβ antibody immobilized on biosensor surface. Based on the synergistic effect of Mn^{2+} and good matched energy level, the immunosensor achieved high sensitivity to

Aβ detection with a broad liner range of 0.2 pg mL^{-1}–50 ng mL^{-1} with a detection limit of 0.068 pg mL^{-1}. Moreover, the resulting immunosensor for quantitative detection of Aβ possesses excellent stability and satisfactory reproducibility. Simultaneously, the enhanced sensitization system may offer a promising method for Aβ detection in clinical diagnostics and provide a potential application for other disease biomarker detection.

Acknowledgements

This study was supported by the National Natural Science Foundation of China 21775053, The Natural Science Foundation of Shandong Province (No.ZR2017MB027), National Natural Science Foundation of China (Nos. 21627809, 21575050, 21505051), and QW thanks the Special Foundation for Taishan Scholar Professorship of Shandong Province and UJN (No.ts20130937).

Appendix A. Supplementary material

Supplementary data associated with this article can be found in the online version at doi:10.1016/j.bios.2018.09.030.

References

Amano, F., 2008. J. Phys. Chem. C 112 (25), 9320–9326.
Amano, F., Yamakata, A., Nogami, K., Osawa, M., Ohtani, B., 2011. J. Phys. Chem. C 115 (33), 16598–16605.
Andreasen, N., Hesse, C., Davidsson, P., Minthon, L., Wallin, A., Winblad, B., Vanderstichele, H., Vanmechelen, E., Blennow, K., 1999. Arch. Neurol. 56 (6), 673–680.
Barghorn, S., Nimmrich, V., Striebinger, A., Krantz, C., Keller, P., Janson, B., Bahr, M., Schmidt, M., Bitner, R.S., Harlan, J., Barlow, E., Ebert, U., Hillen, H., 2005. J. Neurochem. 95 (3), 834–847.
Caballero, L., Mena, J., Morales-Alvarez, A., Kogan, M.J., Melo, F., 2015. Langmuir 31 (1), 299–306.
Carneiro, P., Loureiro, J., Delerue-Matos, C., Morais, S., do Carmo Pereira, M., 2017. Sens. Actuators B-Chem. 239, 157–165.
Chen, S., Nan, H., Zhang, X., Yan, Y., Zhou, Z., Zhang, Y., Wang, K., 2017. J. Mater. Chem. B 5 (20), 3718–3727.
Cong, X., Fan, G.-C., Wang, X., Abdel-Halim, E.S., Zhu, J.-J., 2016. J. Mater. Chem. B 4 (36), 6117–6124.
Fan, D., Wang, H., Khan, M.S., Bao, C., Wang, H., Wu, D., Wei, Q., Du, B., 2017. Biosens. Bioelectron. 97, 253–259.
Gu, W., Gong, S., Zhou, Y., Xia, Y., 2017. Biosens. Bioelectron. 90, 487–493.
Han, Q., Wang, R., Xing, B., Chi, H., Wu, D., Wei, Q., 2018. Biosens. Bioelectron. 106, 7–13.
Jiang, H.-Y., Liu, J., Cheng, K., Sun, W., Lin, J., 2013. J. Phys. Chem. C 117 (39), 20029–20036.
Kang, Q., Yang, L., Chen, Y., Luo, S., Cai, Q., Wen, L., Yao, S., 2010a. Anal. Chem. 82, 9749–9754.
Kang, Q., Yang, L., Chen, Y., Luo, S., Wen, L., Cai, Q., Yao, S., 2010b. Anal. Chem. 82 (23), 9749–9754.
Kaushik, A., Jayant, R.D., Tiwari, S., Vashist, A., Nair, M., 2016. Biosens. Bioelectron. 80, 273–287.
Ke, H., Sha, H., Wang, Y., Guo, W., Zhang, X., Wang, Z., Huang, C., Jia, N., 2017. Biosens. Bioelectron. 100, 266–273.
Li, J., Zhang, Y., Kuang, X., Wang, Z., Wei, Q., 2016. Biosens. Bioelectron. 85, 764–770.
Liang, Y., Guo, N., Li, L., Li, R., Ji, G., Gan, S., 2015. Appl. Surf. Sci. 332, 32–39.
Liu, L., Hensel, J., Fitzmorris, R.C., Li, Y., Zhang, J.Z., 2009. J. Phys. Chem. Lett. 1 (1), 155–160.
Liu, L., Chang, Y., Yu, J., Jiang, M., Xia, N., 2017. Sens. Actuators, B-Chem. 251, 359–365.
Liu, Y., Li, R., Gao, P., Zhang, Y., Ma, H., Yang, J., Du, B., Wei, Q., 2015. Biosens. Bioelectron. 65, 97–102.
Meda, L., Cassatella, M.A., Szendrei, G.I., Otvos, Jr, Baron, P., Villalba, M., Ferrari, D., Rossi, F., 1995. Nature 374 (6523), 647–650.
Mustafa, M.K., Nabok, A., Parkinson, D., Tothill, I.E., Salam, F., Tsargorodskaya, A., 2010. Biosens. Bioelectron. 26 (4), 1332–1336.
Ong, W.L., Natarajan, S., Kloostra, B., Ho, G.W., 2013. Nanoscale 5 (12), 5568–5575.
Qin, J., Jo, D.G., Cho, M., Lee, Y., 2018. Biosens. Bioelectron. 113, 82–87.
Ren, X., Yan, J., Wu, D., Wei, Q., Wan, Y., 2017a. ACS Sens. 2 (9), 1267–1271.
Ren, X., Zhang, T., Wu, D., Yan, T., Pang, X., Du, B., Lou, W., Wei, Q., 2017b. Biosens. Bioelectron. 94, 694–700.
Ren, X., Wu, D., Ge, R., Sun, X., Ma, H., Yan, T., Zhang, Y., Du, B., Wei, Q., Chen, L., 2018. Nano Res. 4, 1–10.
Rushworth, J.V., Ahmed, A., Griffiths, H.H., Pollock, N.M., Hooper, N.M., Millner, P.A., 2014. Biosens. Bioelectron. 56, 83–90.
Su, J., Guo, L., Bao, N., Grimes, C.A., 2011. Nano Lett. 11 (5), 1928–1933.
Sun, L., Xiang, L., Zhao, X., Jia, C.-J., Yang, J., Jin, Z., Cheng, X., Fan, W., 2015. ACS Catal. 5 (6), 3540–3551.
Tian, G., Gu, Z., Zhou, L., Yin, W., Liu, X., Yan, L., Jin, S., Ren, W., Xing, G., Li, S., 2012. Adv. Mater. 24 (9), 1226–1231.
Wang, G.L., Xu, J.J., Chen, H.Y., Fu, S.Z., 2009. Biosens. Bioelectron. 25 (4), 791–796.
Wang, P., Li, D., Chen, J., Zhang, X., Xian, J., Yang, X., Zheng, X., Li, X., Shao, Y., 2014. Appl. Catal. B 160–161, 217–226.
Wang, X., Xu, R., Sun, X., Wang, Y., Ren, X., Du, B., Wu, D., Wei, Q., 2017. Biosens. Bioelectron. 96, 239–245.
Wang, Y., Wang, Y., Wu, D., Ma, H., Zhang, Y., Fan, D., Pang, X., Du, B., Wei, Q., 2018. Sens. Actuators B-Chem. 255, 125–132.
Wei, R.-B., Kuang, P.-Y., Cheng, H., Chen, Y.-B., Long, J.-Y., Zhang, M.-Y., Liu, Z.-Q., 2017. ACS Sustain. Chem. Eng. 5 (5), 4249–4257.
Wen, G., Ju, H., 2016. Anal. Chem. 88 (16), 8339–8345.
Wetchakun, N., Chaiwichain, S., Inceesungvorn, B., Pingmuang, K., Phanichphant, S., Minett, A.I., Chen, J., 2012. ACS Appl. Mater. Interfaces 4 (7), 3718–3723.
Wu, D., Wei, Y., Ren, X., Ji, X., Liu, Y., Guo, X., Liu, Z., Asiri, A.M., Wei, Q., Sun, X., 2018. Adv. Mater. 30 (9), 1705366–1705372.
Xing, B., Zhu, W., Zheng, X., Zhu, Y., Wei, Q., Wu, D., 2018. Sens. Actuators B-Chem. 265, 403–411.
Xu, Q., Zhang, Y., Tang, B., Zhang, C.Y., 2016. Anal. Chem. 88 (4), 2051–2058.
Yang, L., Zhu, W., Ren, X., Khan, M.S., Zhang, Y., Du, B., Wei, Q., 2017. Biosens. Bioelectron. 91, 842–848.
Zang, Y., Lei, J., Hao, Q., Ju, H., 2016. Biosens. Bioelectron. 77, 557–564.
Zang, Y., Lei, J., Ju, H., 2017. Biosens. Bioelectron. 96, 8–16.
Zhang, K., Lv, S., Lin, Z., Tang, D., 2017. Biosens. Bioelectron. 95, 34–40.
Zhang, X., Guo, Y., Liu, M., Zhang, S., 2013. RSC Adv. 3 (9), 2846–2857.
Zhao, H., Fei, H., Hou, J., Liu, Z., Qiang, W., Cao, H., Jing, Q., Peng, S., Cao, G., 2016. ACS Appl. Mater. Interfaces 8 (40), 26675–26683.
Zhao, W.W., Yu, P.P., Shan, Y., Wang, J., Xu, J.J., Chen, H.Y., 2012. Anal. Chem. 84 (14), 5892–5897.
Zhao, W.W., Xu, J.J., Chen, H.Y., 2017. Biosens. Bioelectron. 92, 294–304.